J Neurophysiol 95: 2492–2500, 2006.
First published December 14, 2005; doi:10.1152/jn.01135.2004.

Histamine Excites Neonatal Rat Sympathetic Preganglionic Neurons In Vitro Via Activation of H_1 Receptors

Andrew D. Whyment,[1] Andrew M. Blanks,[1] Kevin Lee,[1] Leo P. Renaud,[2] and David Spanswick[1]
[1]*Warwick Medical School, University of Warwick, Coventry, United Kingdom;* [2]*Neurosciences, Ottawa Health Research Institute, Ottawa, Ontario, Canada*

Submitted 3 November 2004; accepted in final form 9 December 2005

Whyment, A. D., Andrew M. Blanks, Kevin Lee, Leo P. Renaud, and David Spanswick. Histamine excites neonatal rat sympathetic preganglionic neurons in vitro via activation of H_1 receptors. *J Neurophysiol* 95: 2492–2500, 2006. First published December 14, 2005; doi:10.1152/jn.01135.2004. The role of histamine in regulating excitability of sympathetic preganglionic neurons (SPNs) and the expression of histamine receptor mRNA in SPNs was investigated using whole-cell patch-clamp electrophysiological recording techniques combined with single-cell reverse transcriptase polymerase chain reaction (RT-PCR) in transverse neonatal rat spinal cord slices. Bath application of histamine (100 μM) or the H_1 receptor agonist histamine trifluoromethyl toluidide dimaleate (HTMT; 10 μM) induced membrane depolarization associated with a decrease in membrane conductance in the majority (70%) of SPNs tested, via activation of postsynaptic H_1 receptors negatively coupled to one or more unidentified K^+ conductances. Histamine and HTMT application also induced or increased the amplitude and/or frequency of membrane potential oscillations in electrotonically coupled SPNs. The H_2 receptor agonist dimaprit (10 μM) or the H_3 receptor agonist imetit (100 nM) were without significant effect on the membrane properties of SPNs. Histamine responses were sensitive to the H_1 receptor antagonist triprolidine (10 μM) and the nonselective potassium channel blocker barium (1 mM) but were unaffected by the H_2 receptor antagonist tiotidine (10 μM) and the H_3 receptor antagonist, clobenpropit (5 μM). Single cell RT-PCR revealed mRNA expression for H_1 receptors in 75% of SPNs tested, with no expression of mRNA for H_2, H_3, or H_4 receptors. These data represent the first demonstration of H_1 receptor expression in SPNs and suggest that histamine acts to regulate excitability of these neurons via a direct postsynaptic effect on H_1 receptors.

INTRODUCTION

Histamine (β-imidazolylethylamine) is an endogenous, biogenic amine that is known to mediate numerous physiological processes (Hough 1988; Schwartz et al. 1991; Wada et al. 1991). Histamine is widely distributed throughout the mammalian CNS (Hill 1990; Schwartz et al. 1991; Yamatodani et al. 1991), with histaminergic axons arising almost exclusively from the tuberomammillary nucleus of the posterior hypothalamus, from which efferent fibers project to almost all areas of the brain (Schwartz et al. 1991; Takada et al. 1987; Wada et al. 1991) and spinal cord (Schwartz et al. 1991; Wahlestedt et al. 1985). Extensive pharmacological and molecular analysis has identified at least four subtypes of histamine receptor (H_1–H_4, see Haas and Panula 2003). Three of the four histamine receptors that have been identified (H_1–H_3) are prominently expressed in the CNS in specific cellular compartments (Agulló et al. 1990; Inagaki 1989), whereas the fourth (H_4) receptor (Nguyen et al. 2001) is detected predominantly in the periphery, for example, in bone marrow and leukocytes (Liu et al. 2001; Oda and Matsumoto 2001; Shin et al. 2002). Consistent with this diffuse distribution, neuronal histamine is capable of inducing a wide variety of cellular effects via its receptors (Mitsuhashi and Payan 1992).

Histamine is indicated as being involved in modulating numerous autonomic functions. For example, in the periphery histamine excites neurons in the sympathetic superior cervical ganglion (Christian et al. 1989; Snow and Weinreich 1987) and histamine modulates sympathetic postganglionic synaptic transmission via a presynaptic action at H_1 and H_3 receptors (Christian and Weinreich 1992). Histamine also excites vagal afferent neurons (Higashi et al. 1982; Leal-Cardoso et al. 1993; Undem and Weinreich 1993; Undem et al. 1993), in part by inhibition of intrinsic potassium conductances (Jafri et al. 1997). In addition to this peripheral role, histamine has also been indicated as regulating autonomic function centrally, including activation of the sympathetic nervous system (see Brown et al. 2001; Yasuda et al. 2004). However, to our knowledge, only supraspinal hypothalamic and brain stem sites, antecedent to the origins of the sympathetic outflow in the spinal cord, have been explored. Descending histaminergic inputs to the spinal cord originating in the tuberomammilary nucleus are well documented (Schwartz et al. 1991; Wahlestedt et al. 1985), although the precise neural compartments targeted and the physiological functions regulated at this level are unclear. To investigate the potential role of histamine in regulating autonomic function at the level of the spinal cord, we used whole-cell patch-clamp electrophysiological recording techniques combined with single-cell reverse transcriptase polymerase chain reaction (RT-PCR) to investigate the effects of histamine on SPNs in the intermediolateral cell column. These neurons are the most important final central site for integration of sympathetic autonomic reflexes and the origins of the sympathetic outflow for control of vascular and visceral function (Coote 1988). Here we report for the first time that histamine acts to directly excite SPNs by engaging postsynaptic H_1 receptors, negatively coupled to one or more K^+ conductances.

Address for reprint requests and other correspondence: D. Spanswick, Warwick Medical School, University of Warwick, Coventry, CV4 7AL, United Kingdom. (E-mail: D.C.Spanswick@warwick.ac.uk).

The costs of publication of this article were defrayed in part by the payment of page charges. The article must therefore be hereby marked "*advertisement*" in accordance with 18 U.S.C. Section 1734 solely to indicate this fact.

METHODS

Slice preparation

Electrophysiological recordings were made from transverse thoracolumbar spinal cord slices as described previously (Logan et al. 1996; Pickering et al. 1991). Briefly, Wistar Kyoto rats, ages 6–14 days (either sex), were terminally anesthetized using 4% Enflurane in O_2 (Abbott Laboratories, Queensborough, Kent, UK) and decapitated. The spinal cord was removed and thoracic sections were cut into 300–400 μm thick slices using a Leica VT1000 S (Leica Microsystems UK, Milton Keynes, United Kingdom). Slices were maintained in artificial cerebrospinal fluid (aCSF) at room temperature for 1 h after slicing before experimentation was performed. For recording, individual slices were held between two grids in a custom-built chamber continuously perfused with aCSF at a rate of 4–10 ml min^{-1}, illuminated from below, and viewed under a dissection microscope. The aCSF was of the following composition (mM): NaCl, 127, KCl, 1.9, KH_2PO_4, 1.2, $CaCl_2$, 2.4, $MgCl_2$, 1.3, $NaHCO_3$, 26, D-glucose, 10, equilibrated with 95% O_2-5% CO_2.

Cell identification

SPNs were identified by their characteristic electrophysiological properties: a long-duration action potential (5–10 ms) with a shoulder on the repolarization phase, a large-amplitude (18–30 mV) and prolonged action potential afterhyperpolarization, and the expression of inwardly rectifying and transient outwardly rectifying conductances (Logan et al. 1996; Pickering et al. 1991). The neuronal morphology was also routinely determined retrospectively with lucifer yellow (CH dipotassium salt, 1 $mg.ml^{-1}$, Sigma) or biocytin (5 mM, Sigma) in the patch pipette solution. Methods for visualizing filled SPNs have been reported in detail previously (see Pickering et al. 1991 for Lucifer yellow and Spanswick et al. 1998 for biocytin).

Recordings

Whole cell recordings were performed at room temperature (17–21°C) from neurons in the intermediolateral cell column with an Axopatch 1D amplifier (Axon Instruments, Foster City, CA.), using the blind version of the patch-clamp technique (Pickering et al. 1991). Patch pipettes were pulled from thin-walled borosilicate glass (GC150-TF10, Clarke Electromedical, Pangbourne, Berkshire, United Kingdom) and had resistances of between 3 and 8 MΩ when filled with intracellular solution of the following composition (mM): potassium gluconate, 130, KCl, 10, $MgCl_2$, 2; $CaCl_2$, 1, EGTA-Na, 1, HEPES, 10, Na_2ATP, 2, and Lucifer yellow, 2 (or biocytin, 5), pH adjusted to 7.4 with KOH, osmolarity adjusted to 310 $mosmol^{-1}$ with sucrose.

Series resistance compensation of approximately 70–80% was applied for whole-cell voltage clamp experiments. Access resistance ranged between 5 and 25 MΩ. Neuronal input resistances were measured by injecting small, rectangular-wave, hyperpolarizing current pulses of constant amplitude (–10 to −100 pA) and measuring the mean amplitude of a minimum of five resulting electrotonic potentials, in control conditions and in the presence of the test compound. Recordings were monitored on an oscilloscope (Gould 1602, Gould Instrument Systems), displayed on a chart recorder (Gould, Easygraf TA240), and stored on digital audio tapes (Biologic, DTR-1205) for later off-line analysis. In addition, data were filtered at 2–5 kHz, (1 kHz for voltage clamp data), digitized at 2–10 kHz (Digidata 1322, Axon Instruments) and stored on a PC running pCLAMP 8.2 data acquisition software. Analysis of electrophysiological data was carried out using Clampfit 8.2 software (Axon Instruments).

Cell harvest and single-cell RT-PCR

The SPN cytoplasm was gently aspirated under visual control into a patch-clamp recording electrode. The contents of the electrode were subsequently dissipated into a microtube and reverse transcribed in a reaction volume of 10 μl containing 1× first-strand buffer, 0.1 M DTT, 10 mM dNTP, 1.5 U RNAsin (Promega, Southampton, United Kingdom), 200 U Superscript II reverse transcriptase (Invitrogen, Paisley, United Kingdom), and 0.5 ng reverse transcription primer for 60 min at 42°C. Three prime end amplification (TPEA) was performed (Richardson et al. 2000). Briefly, the RT primer was composed of an anchored oligo(dT) primer with a specific 5′ heel sequence: 5′-GACTGCCAGACCGCGCGCCTGACGCGTAATACGACTCAC TATAGGGTTTTTTTTTTTTTTTTTT-3′. Second-strand cDNA synthesis was initiated by incubation of the first-strand cDNA with 1 ng of a primer consisting of 5′-AAAACTG CCAGACCGCGCGCCTGAACGCGTCGTATTAACCCTCACTA-AAGGGNNNNNNNNNNNNNN-3′ (where N represents C, G, T or A) during PCR amplification for 29 cycles, 10 s annealing (50°C), 2.5 min extension (72°C), and 1 min denaturing (94°C). After the initial round, further amplification was performed by the addition of 230 ng heel primer consisting of 5′-ACTGCCAGACCGCGCGC-CTGA-3′. Samples of amplified cDNA were diluted 1:10 and subjected to hot-lid PCR carried out in a total reaction volume of 25 μl. Reaction components were as follows: 2.5 μl 10 x PCR buffer, 1 μl 25 μM 5′ primer, 1 μl 25 μM 3′ primer, 1 μl 25 mM $MgCl_2$, 0.5 μl 10 mM dNTP, 12.5 μl 2.6 mM Betaine/2.6% DMSO, 4.25 μl H_20, 0.25 μl Platinum *Taq* polymerase (Invitrogen, Paisley, United Kingdom). Amplifications were carried out on a PTC-225 thermal cycler (Tetrad, MJ Research). Following an initial 4-min denaturing step (95°C), each PCR cycle consisted of 30 s denaturing (94°C), 30 s annealing (60°C), and 20 s extension (72°C). After the final cycle, the reaction was held for 5 min at 72°C. The PCR products were then separated on an ethidium bromide-stained 2% agarose gel and photographed. Direct sequencing was performed to confirm the identity of the amplified products. All gene-specific primers are listed in Table 1.

Statistical analyses

Statistical analysis was performed using Excel 2003 (Microsoft) and Prism 4 (Graphpad), with all values given as means ± SE. Statistical significance was determined using 2-tailed Mann-Whitney *U* tests. $P < 0.05$ was taken to indicate statistical significance.

Drugs

The following drugs were used: clobenpropit dihydrobromide (10 μM), dimaprit dihydrochloride (10 μM), histamine (100 μM), HTMT (10 μM), imetit dihydrobromide (100 nM), tiotidine (5 μM), and *trans*-triprolidine hydrochloride (triprolidine, 100 μM), all from Tocris Cookson, and tetrodotoxin (TTX, 500 nM) from Alomone Laboratories, Israel.

Tiotidine was prepared as a stock solution using DMSO (Sigma) and diluted to the required concentration in aCSF immediately prior to use. Final DMSO concentrations did not exceed 0.1%, and appropriate vehicle controls were performed, which were without effect. All other drugs were made as stock solutions in distilled water. The drugs were administered to the slice by perfusion from 50-ml syringes arranged in line with the main aCSF reservoir by a series of three-way valves. The reported agonist final concentrations represent the concentrations within the perfusion system and do not take into account dilution within the recording chamber. Antagonists were applied for ≥10 min prior to the addition of agonists to ensure complete equilibration within the recording chamber.

RESULTS

Whole cell recordings from 47 neurons, identified as SPNs on the basis of their characteristic morphology and electrophysiological properties were included in this study. Morphology was revealed with either Lucifer yellow or biocytin,

TABLE 1. *Gene-specific primers used for single-cell RT-PCR*

Name	Gene Accession Number	Primer Sequence (+), sense; (−), antisense	Product length, bp
H_1 receptor	D12800	(+) 5′-CAAAGGAAAAGAGGTTCCTGG-3′	202
		(−) 5′-GTCACCCTCTGTGGACAGGT-3′	
H_2 receptor	S57565	(+) 5′-GGTTGAACAACTCTCTGCTGC-3′	221
		(−) 5′-CCTAAGAGAGCCAGCCATTG-3′	
H_3 receptor	AY009371	(+) 5′-CCGTACACGCTCCTAATGAT-3′	135
		(−) 5′-GTAGTGGCACAGTGGGTAGAG-3′	
H_4 receptor	NM131909	(+) 5′-TGCCAGCTTCTGTCTCTGTC-3′	147
		(−) 5′-ACTGCTGTTGGCTCGTGTTC-3′	
β-actin	V01217	(+) 5′-CATCCATGCCCTGAGTCC-3′	207
		(−) 5′-ACACCTCAAACCACTCCCAG-3′	
Intron	see Telenius *et al.* 1992	(+) 5′-GTGGATATAGTTGAGTCC-3′	
		(−) 5′-CACATGTTGACCACTCCAT-3′	

revealing somata located within the lateral horn, medially projecting dendrites, and an axon that coursed toward the ventral horn (see Spanswick et al. 1998). The characteristic electrophysiological profile of an SPN included a relatively long duration (5–10 ms) action potential with a distinct shoulder in the repolarizing phase, large amplitude (18–30 mV) afterhyperpolarization, and transient outward rectification observed as a delay in the return to rest of the voltage response following a series of hyperpolarizing current pulses (Spanswick et al. 1998). The neurons had a mean resting membrane potential of −49.9 ± 5.8 mV and a mean resting input resistance of 523 ± 61 MΩ.

The effects of histamine receptor agonists on SPN

Histamine (100 μM, $n = 23$), the H_1 receptor agonist HTMT dimaleate (10 μM, $n = 12$), the H_2 receptor agonist dimaprit dihydrochloride (10 μM, $n = 5$), or the H_3 receptor agonists imetit dihydrobromide (100 nM, $n = 4$) were bath applied to the slice by superfusion for 15–120 s. Bath application of histamine induced membrane depolarization in 16/23 SPNs tested (69.6%, Fig. 1*Aa*). The response was characterized by depolarization of the membrane from a mean resting or holding potential of −48.6 ± 1. 9mV to −44.1 ± 2.2 mV, and a mean peak membrane depolarization of 4.5 ± 0.6 mV ($n = 16$, Fig. 1*B*). The histamine-induced membrane depolarization was associated with a concurrent increase in neuronal input resistance from a mean of 462 ± 43 MΩ at rest to 540 ± 41 MΩ in the presence of histamine, amounting to a 16.9 ± 3.0% increase (Figs. 2*Ab* and 5, *Aa* and *Ac*). In the remaining seven cells, no significant changes in either membrane potential or neuronal input resistance were observed.

Application of HTMT induced membrane depolarization in 9/12 cells tested (75%, Fig. 1*Ab*), from a mean resting value of −49.3 ± 2.0 mV to −45.5 ± 2.4 mV, and a mean peak membrane depolarization of 3.9 ± 0.5 mV ($n = 9$, Fig. 1*B*). This depolarization was again associated with a significant increase in neuronal input resistance from a resting value of 418 ± 51 MΩ to 468 ± 59 MΩ, amounting to a 12.1 ± 1.5% increase (Fig. 1*B*). Dimaprit ($n = 5$) or imetit ($n = 4$) had no statistically significant effect on either membrane potential or input resistance (Fig. 1*B*). All responses persisted in the presence of TTX (500 nM; $n = 5$) and were, for the main part, fully reversible on wash (Fig. 2*Ab*).

The effects of histamine receptor antagonists on agonist-induced responses

Application of triprolidine (10 μM, $n = 7$), a specific antagonist of the H_1 receptor, induced a reversible inhibition of the membrane depolarization induced by histamine (Fig. 2*Ac*). In the presence of triprolidine, the peak amplitude of histamine-induced membrane depolarization was reduced by 86.7 ± 6.7%, from 4.5 ± 0.6 mV to 0.6 ± 0.4 mV in the presence of the H_1 receptor antagonist ($P < 0.03$, Fig. 2*B*). A similar effect of triprolidine was observed on histamine-induced changes in input resistance. This amounted to an 84.5 ± 17.4% ($P < 0.01$) reduction in the associated input resistance change induced by histamine in the presence of triprolidine (16.7 ± 2.6 MΩ increase in control conditions compared with a 2.6 ± 1.1 MΩ increase in the presence of the antagonist, $P < 0.03$, Fig. 2*B*). Conversely, application of the specific H_2 receptor antagonist, tiotidine (10 μM, $n = 4$), had no significant effect on either the membrane depolarization or change in neuronal input resistance induced by histamine (Fig. 2*B*). Likewise, application of clobenpropit (5 μM, $n = 5$), a specific antagonist of the H_3 receptor, had no significant effect on the membrane depolarization or increase in input resistance induced by histamine (Fig. 2*Ad* and *B*).

Ionic mechanism underlying the histamine H_1 receptor-mediated depolarization

The H_1 receptor-mediated depolarization was associated with an increase in neuronal input resistance. Thus experiments were undertaken to elucidate the ionic mechanism underlying the H_1 receptor-mediated depolarization. One likely mechanism underpinning membrane depolarization associated with a reduction in input conductance is closure of one or more resting membrane potassium conductances. Thus the actions of the nonselective potassium channel blocker barium ($BaCl_2$) on the histamine-induced membrane depolarization were examined. Bath application of $BaCl_2$ (1 mM, $n = 4$), a concentration previously demonstrated to be sufficient to block potassium conductance's contributing to resting membrane potential in SPN (Spanswick and Renaud, unpublished observations), induced a 3 mV membrane potential depolarization and induced action potential discharge in previously silent neurons, therefore mimicking the effects of histamine. On subsequent injection of hyperpolarizing current to hold the neuron below its

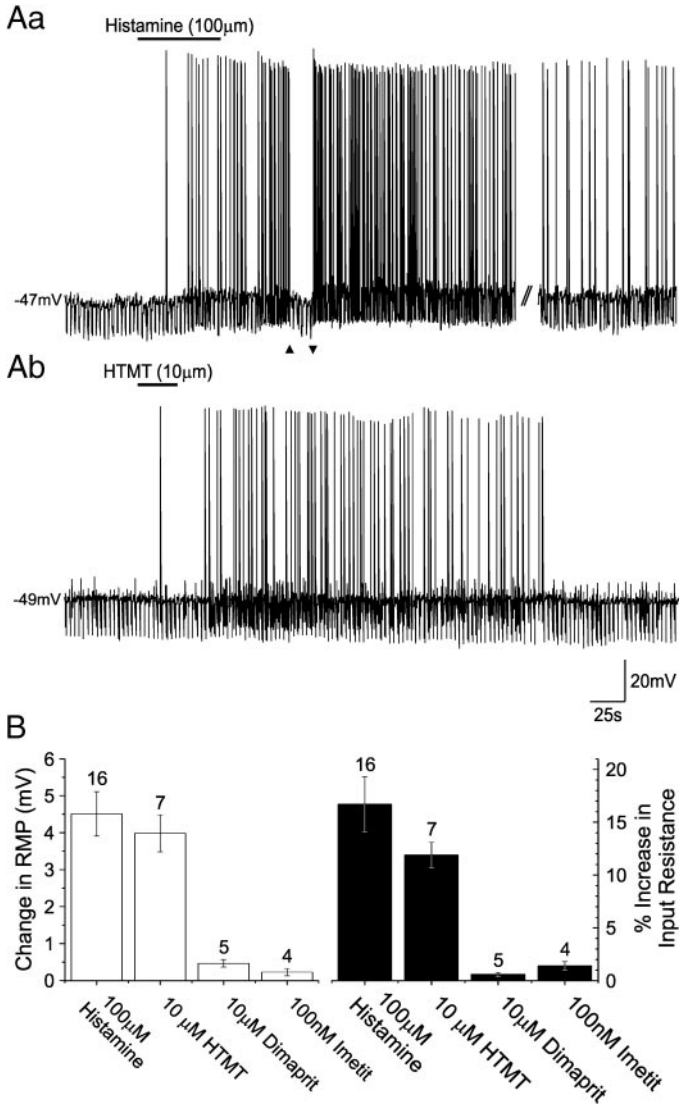

FIG. 1. SPNs express functional postsynaptic H_1 receptors. *Aa*: samples of a continuous whole-cell current-clamp recording from an SPN with a resting membrane potential of −47 mV, showing histamine-induced depolarization and concomitant increase in neuronal input resistance, indicated by the increase in amplitude of electrotonic potentials (downward deflections of the records) evoked in response to hyperpolarizing rectangular wave current pulses (not shown). Constant negative current was injected to monitor the change in input resistance at the resting membrane potential of the neuron and to negate the effect of any voltage-dependent channels. The start and end of the constant current injection are marked by ▲ and ▼ respectively. Double slashes indicate a break in the trace of 60 s. *Ab*: samples of a continuous whole-cell current-clamp recording from another SPN showing membrane depolarization and increased action potential firing rate on application of the H_1 receptor specific agonist, HTMT. The response was fully reversible. *B*: summary histogram illustrating the profile of histamine receptor-mediated responses evoked in SPN. The change in peak membrane potential (open columns) and neuronal input resistance (filled columns) responses to histamine and the specific histamine-receptor agonists are shown. Error bars represent SE. Numbers above individual bars indicate number of cells tested (*n*).

firing threshold in the presence of $BaCl_2$, application of histamine was without significant effect on either membrane potential or input resistance (Fig. 3*Ab*). On wash of $BaCl_2$, subsequent application of histamine induced membrane depolarization (Fig. 3*Ac*), suggesting involvement of one or more K^+ conductances in histamine-induced depolarization.

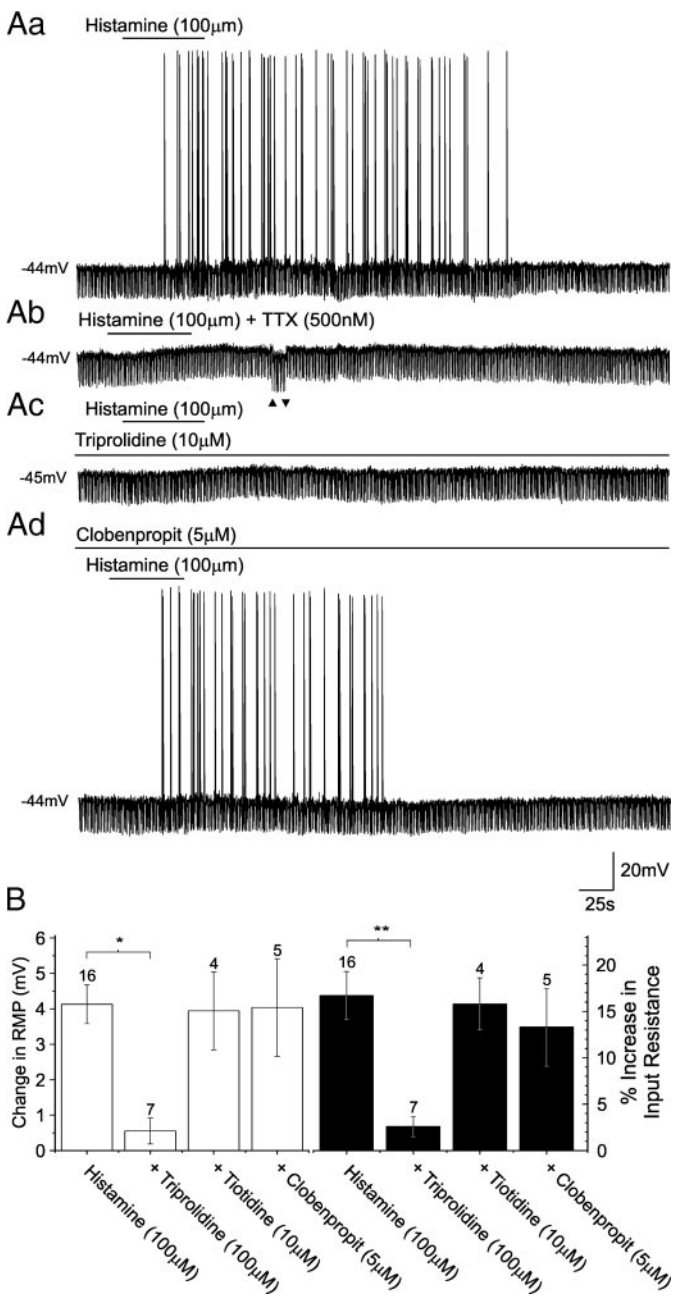

FIG. 2. Histamine-induced membrane responses are blocked by H_1, but not H_2 or H_3, receptor antagonists. *Aa*: samples of a continuous whole-cell current-clamp recording from an SPN with a resting membrane potential of −44 mV, showing histamine-induced depolarization and concomitant increase in firing rate. *Ab*: samples of a continuous whole-cell current-clamp recording from the same neuron shown in *Aa* in the presence of TTX (500 nM). Application of histamine induced membrane depolarization and an increase in input resistance, which was compared before and during the response to histamine at similar membrane potentials, maintained in the presence of histamine by injection of constant negative current. The start and end of the current injection are marked by ▲ and ▼, respectively. *Ac*: application of the H_1 receptor specific antagonist triprolidine significantly reduced the histamine-induced depolarization and input resistance change. *Ad*: the H_2 receptor-specific antagonist clobenpropit was without effect on the histamine-induced membrane responses. *B*: summary histogram illustrating the pharmacological profile of histamine receptor-mediated responses evoked in SPNs. The peak membrane potential (open columns) and neuronal input resistance (filled columns) responses to histamine and the specific histamine-receptor antagonists are shown. Error bars represent SE. Numbers above individual bars indicate number of cells tested (n). (* $P < 0.01$, ** $P < 0.03$).

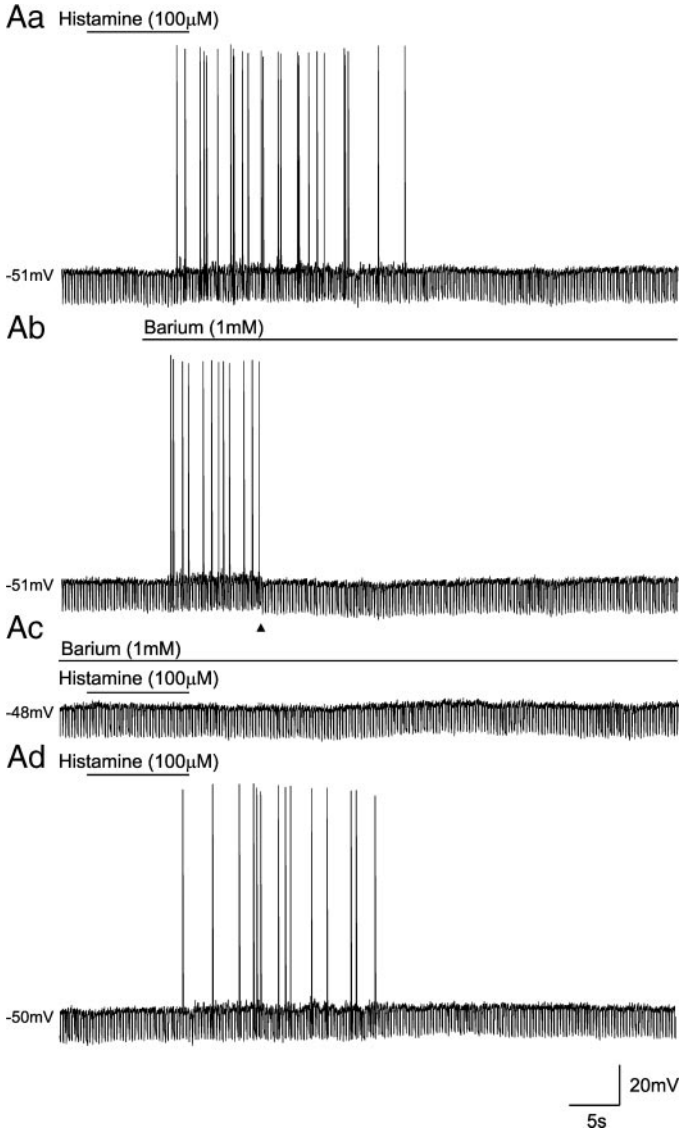

FIG. 3. Histamine-induced membrane responses are blocked by barium. *Aa*: samples of a continuous whole cell current-clamp recording from an SPN, showing that application of histamine induced membrane depolarization and an increase in neuronal firing rate. *Ab*: in the same neuron shown in *Aa*, application of the broad spectrum K^+ channel blocker barium (1 mM) induced membrane depolarization and action potential discharge. ▲ indicates the start of constant hyperpolarizing current injection to clamp the neuron to its resting membrane potential. Note the increase in input resistance. *Ac*: continuation of the trace shown in *Ab*, showing that barium blocked the membrane responses induced by histamine. *Ad*: the effects of the barium were reversible on wash.

To further clarify the ionic mechanism underlying histamine-induced excitation of SPNs, we performed a series of experiments to identify the reversal potential and thus the ions mediating the response. In voltage clamp at a holding potential of −60 mV, application of histamine (100 μM, 60 s, $n = 4$) induced a sustained inward current, with a mean peak amplitude of 18.7 ± 3.9 pA (Fig. 4*Aa*). Voltage ramps from −120 to −60 mV at a rate of 10 mVs^{-1} were applied in control conditions and at the peak of the histamine-induced response to investigate the reversal potential of the histamine-induced current (Fig. 4*Ab*). Histamine-induced inward currents had a mean reversal potential of −93 ± 5.9 mV ($n = 4$), close to the K^+ reversal potential under our recording conditions (Fig.

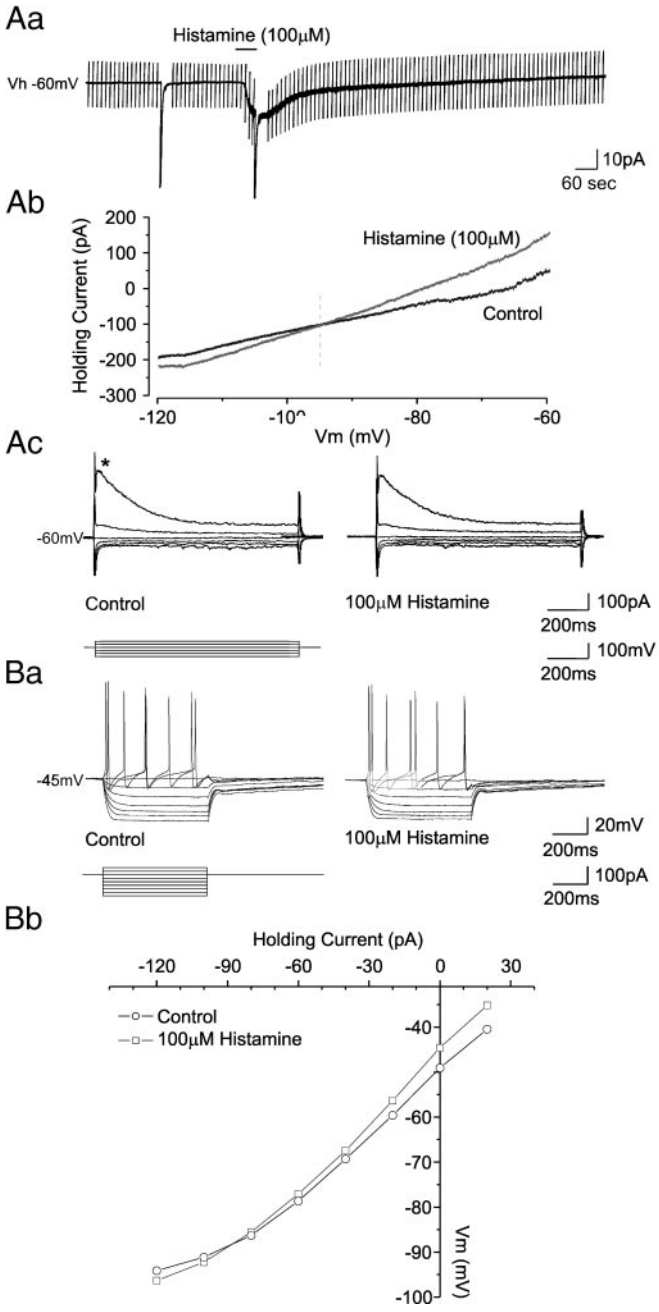

FIG. 4. Ionic mechanism underlying histamine-induced membrane responses in SPNs. *Aa*: Whole cell voltage-clamp recording (V_h −60 mV) showing that application of histamine produced a pronounced inward current. Large downward deflections represent current responses to voltage ramps from −120 to −60 mV (10 mVs^{-1}), shown on a faster time base, superimposed in *b*. Note that the reversal potential for the histamine-induced current is close to the K^+ reversal potential under our recording conditions. *Ac*: superimposed samples of a continuous whole cell voltage-clamp recording showing the lack of effect of histamine on the transient outward current evoked in response to the largest depolarizing voltage step (*). *Ba*: superimposed samples of a continuous whole cell current-clamp recording showing membrane potential responses of an SPN to a series of depolarizing and hyperpolarizing rectangular-wave current pulses before histamine and in the presence of histamine. *Bb*: plot of the current-voltage (*I-V*) relationships before (○) and in the presence of histamine (□), shown in *Ba*. Again, note the increase in the slope of the *I-V* relationship in the presence of histamine indicating an increase in neuronal input resistance, and the reversal potential around −90 mV, close to that for potassium ions under our recording conditions.

4*Ab*). Current-voltage relationships were obtained from seven cells, in control conditions and at the peak of the histamine-induced depolarization (Fig. 4*Ba*). Under these conditions, the histamine-induced conductance change had a reversal potential of -85 ± 4 mV (Fig. 4*Bb*), close to the reversal potential for K^+ ions under our recording conditions. The more depolarized reversal potential in current clamp may reflect a poor control of membrane potential in this recording mode. Previous studies have indicated that histamine regulates A-type potassium currents (Starodub and Wood 2000). However, the prolonged transient outwardly rectifying A-like conductance observed in SPNs in the present study was unaffected by histamine (Fig. 4*Ac*).

Subthreshold oscillations induced by H_1 receptor agonists

Bath application of histamine (100 μM) induced biphasic membrane potential oscillations in 5/17 previously quiescent SPNs at the peak of the histamine-induced membrane depolarization (Fig. 5, *Aa* and *Ab*). These oscillations, characterized by a fast depolarizing transient followed by a slower hyperpolarization, are a feature of electrotonically coupled SPNs and arise from the passive conduction of action potentials from adjoining neurons through electrotonic synapses (Logan et al. 1996; Nolan et al. 1999). In the remaining 12 neurons, histamine-induced depolarization was not associated with the induction of oscillations, presumably reflecting a lack of electrotonic coupling between these neurons. Application of histamine (100 μM) or HTMT (10 μM) to SPNs discharging spontaneous oscillations in membrane potential induced an increase in both the amplitude and frequency of oscillations in three of five cells tested, (Fig. 5, *Ba* and *Bb*), from 9.8 ± 1.2 mV and 0.85 ± 0.13 Hz in control conditions to 17.27 ± 3.4 mV and 2.70 ± 0.37 Hz in the presence of the agonist ($n = 3$, $P < 0.02$ and $P < 0.01$, respectively, for amplitude and frequency).

Single-cell RT-PCR analysis of histamine receptor mRNA expression in SPNs

To further clarify the nature of the histamine receptor(s) expressed by SPN and responsible for the membrane potential depolarization and concurrent increase in neuronal input resistance, we performed single-cell RT-PCR. The cytosolic contents were aspirated from eight neurons, which were subjected to RT-PCR using specific primers for all four histamine receptors, and the housekeeping gene, β-actin (see Table 1).

H_1 receptor mRNA expression was detected in six of the eight cells investigated (75%). No detectable levels of mRNA for the remaining three receptors (H_2, H_3, and H_4) were observed in any of the cells tested (Fig. 6*A* and *B*). Only cells expressing the housekeeping gene β-actin were used in the study, and a negative control was performed, which showed negative expression for all mRNA transcripts tested (Fig. 6*A*).

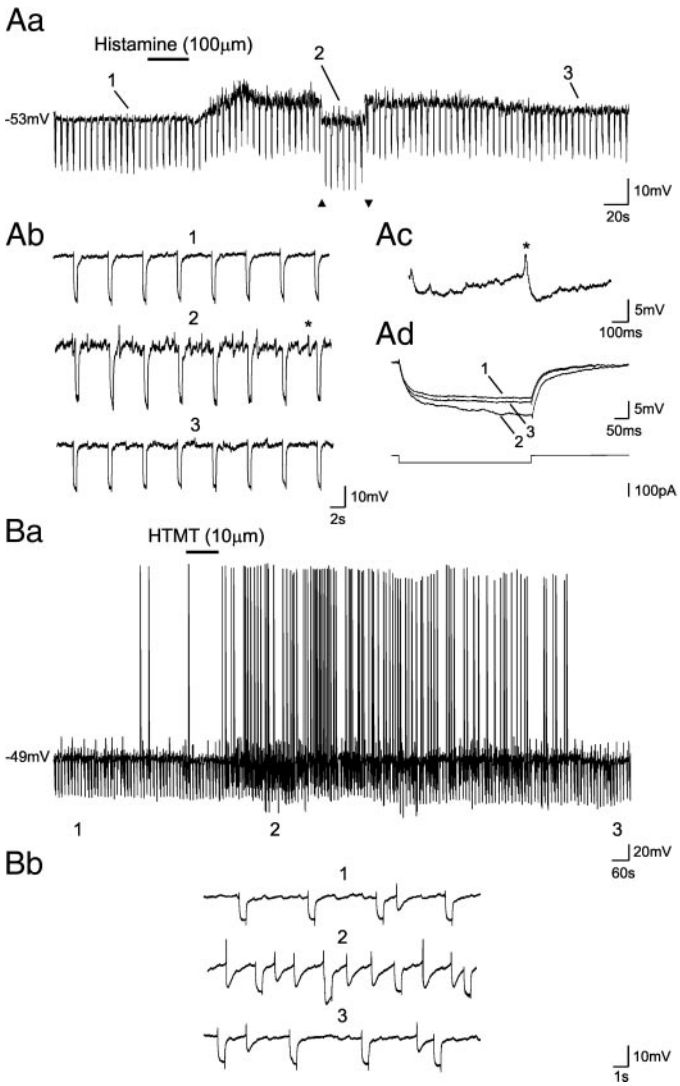

FIG. 5. Histamine-induced membrane potential oscillations in SPNs. *Aa*: continuous whole-cell current-clamp recording from an SPN with a resting membrane potential of -53 mV, showing histamine-induced depolarization. The numbers above the trace indicate the regions shown on an expanded scale in *Ab*. *Ab*: regions of the record shown in *Aa* illustrated on an expanded time scale. Note the appearance of fast transient events in the presence of histamine (2) compared with control and wash (1 and 3, respectively), an example of which is depicted by the * and shown on a faster time-base in *Ac*. *A:* these fast transient events were characterized by a rapid depolarization followed by a slower, more pronounced hyperpolarization. *Ad*: membrane potential deflections in response to negative current injection shown on an expanded scale illustrating the marked increase in input resistance in the presence of histamine (2), compared with control and wash (1 and 3, respectively). Numbers correspond to the sections of traces highlighted in *Ab* from which these membrane responses were taken. The lower trace indicates the injected current pulse used to evoke membrane responses shown above. *Ba*: samples of a continuous whole-cell current-clamp recording from another SPN, showing increased firing frequency in the presence of the H_1 receptor-specific agonist HTMT. Furthermore, similar to histamine, membrane potential oscillations, observed as transient, small-amplitude upward deflections of the record, increased in frequency in the presence of this agonist. The numbers below the trace indicate the regions of the record shown on an expanded timescale in *Bb*. *Bb*: samples of the record shown in *Ba* illustrated on an expanded time scale. Note the increase in the frequency of fast transient oscillations in the presence of HTMT (2) compared with control and wash (1 and 3, respectively).

DISCUSSION

Histamine has been indicated as being involved in a range of homeostatic mechanisms that ultimately involve the engagement of the sympathetic nervous system (see Brown et al. 2001; Yasuda et al. 2004), including energy expenditure and cardiovascular control. For example, a number of studies

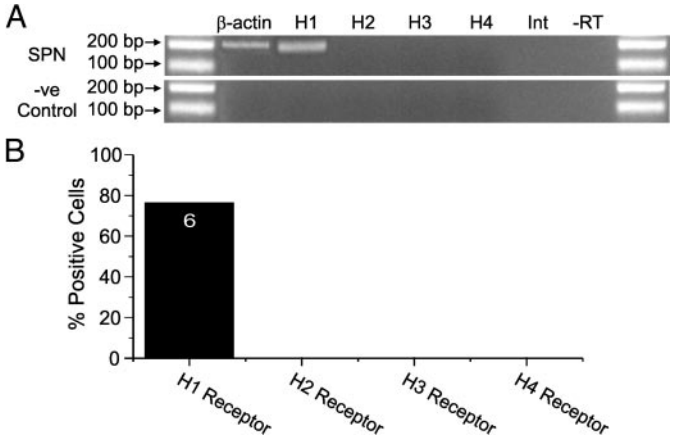

FIG. 6. SPNs express H_1 receptor mRNA. *A*: ethidium bromide stained gels of the scRT-PCR products amplified with primers specific for transcripts indicated by the labels above the appropriate columns. Expression of only the H_1 histamine receptor in addition to the housekeeping gene β-actin mRNA were detected in SPNs. These neurons did not express mRNA for H_2, H_3, or H_4. A negative (-ve) control was performed on the contents of an electrode which was placed next to a cell without seal formation or harvesting of cytoplasmic contents. Molecular weight markers are shown in the lanes on the far left and far right, together with corresponding number of base pairs. (Int, Intronic; -RT, cell contents lacking reverse transcriptase in the PCR amplification process). *B*: summary histogram illustrating the expression of the mRNA transcripts expressed in SPN. Data from eight cells.

indicate that activation of the central histamine system leads to elevated levels of plasma catecholamines (Akins and Bealer 1993; Knigge et al. 1990; Matzen et al. 1992; Okuma et al. 1997) and changes in blood pressure and heart rate (Gatti and Gertner 1983; Klein and Gertner 1981, 1983; Singewald and Phillippu 1996; Tangri et al. 1989). Thus histamine has a role in regulating autonomic function, both peripherally and centrally. However, the only role for histamine in regulating central sympathetic outflow that has been considered to date has been at higher levels in the hypothalamus and brain stem, thus antecedent and supraspinal to SPNs. To our knowledge, there have been no reports of histamine acting directly on the origins of the sympathetic outflow in the spinal cord. Thus the data presented here are the first to indicate a direct role for histamine in the regulation of excitability of SPNs. The major findings are that histamine, through the activation of postsynaptic H_1 receptors negatively coupled to one or more K^+ conductances, acts to excite two thirds of these neurons.

SPN express functional postsynaptic H_1, but not H_2 or H_3, receptors

Bath application of histamine induced membrane depolarization that was associated with an increase in neuronal input resistance in 70% of neurons. Responses persisted in the presence of TTX, indicative of a direct effect on the neuron. This effect was mimicked by the highly selective H_1 receptor agonist HTMT and was blocked by the potent and selective H_1 receptor antagonist triprolidine, confirming the presence of postsynaptic H_1 receptors in the majority of SPNs. This notion was further supported by single-cell RT-PCR data, with mRNA for the H_1 receptor being found in 75% of neurons tested. Agonists and antagonists for either H_2 or H_3 receptors were without effect on SPN. This latter data together with results from single-cell RT-PCR and pharmacological studies yielded no evidence for the expression of H_2, H_3, or H_4 receptors in these neurons. Furthermore, a subpopulation (25%) of SPNs did not express detectable levels of H_1 receptor mRNA. Whether this indicates that histaminergic inputs innervate SPN differentially in a target- and function-specific manner, or that H_1 receptor expression is subject to modulation in a temporal and/or spatial fashion, remains to be determined.

Ionic mechanism underlying histamine-induced depolarization in SPNs

The histamine-induced membrane depolarization and associated increase in neuronal input resistance was barium sensitive and exhibited a reversal potential close to that of K^+ ions under our recording conditions, consistent with the effect of histamine being mediated by closure of one or more potassium-selective conductances. Likewise, in voltage clamp, the histamine-induced inward current had a reversal potential, indicating potassium selectivity. Thus the signal transduction mechanism activated through these receptors ultimately leads to closure of one or more resting potassium conductances and increased excitability of SPNs. Similar mechanisms of action of histamine have been reported in peripheral autonomic neurons, where histamine acting via H_1 receptors excites vagal afferents by blocking a resting leak potassium conductance and a potassium conductance contributing to afterhyperpolarization (Jafri et al. 1997). Similarly in other central neurons, histamine acting via H_1 receptors excites thalamic neurons (McCormick and Williamson 1991), hypothalamic supraoptic neurons (Li and Hatton 1996), striatal cholinergic interneurons (Munakata and Akaike 1994), and cerebral cortical neurons (Reiner and Kamondi 1994). All of these studies on central neurons, as with the SPNs described here, revealed that histamine-induced responses were blocked in the presence of extracellular barium and mediated via inhibition of resting leak potassium conductances. Other potassium conductances targeted by histamine-dependent signaling mechanisms include the M-current (Guo and Schofield 2002) and A-current (Starodub and Wood 2000), although no effect of histamine was observed on the A-like conductance in SPNs in the present study. However, we cannot discount an effect of histamine on D-like conductances in some SPNs in the present study, although this seems unlikely given that we observed no effect of histamine on transient outward rectification in these neurons.

In relation to the signal transduction mechanism, binding of histamine to the H_1 G protein-coupled receptor stimulates phospholipase C (PLC) through activation of the $G_{q/11}$ G protein (Leurs et al. 1994). PLC in turn hydrolyzes phosphatidyl-4, 5-bisphosphate (PIP_2) to form two second messengers, diacyl glycerol (DAG) and inositol triphosphate (IP_3). DAG potentiates the activity of PKC, which can block a leak K^+ conductance ($I_{K(leak)}$) (see Brown et al. 2001; Haas and Panula 2003) that contributes to neuronal resting membrane potential. Although a full investigation of the conductance and signal transduction pathway involved was not performed in the present study, it is tempting to speculate that the excitation induced by histamine in SPNs occurs by means of a block of $I_{K(leak)}$, either directly via activation of $G_{q/11}$ or via subsequent activation of DAG and PKC. Further studies are required to clarify this.

Induction of membrane potential oscillations in SPNs

Biphasic membrane potential oscillations were induced by histamine and the histamine H_1 receptor agonist HTMT in previously quiescent SPNs, and the frequency of oscillations increased in spontaneously active SPNs. Previous studies in SPNs indicated that such oscillations are the hallmark of electrotonic coupling between these neurons (Logan et al. 1996; Nolan et al. 1999). Thus these data suggest that histamine acts to regulate excitability of electrotonically coupled SPNs. In cultured supraoptic neurons, H_1 receptor activation leads to a significant increase in dye coupling, and has been suggested to reflect an increased number of electrical synapses between neurons (Hatton and Yang 1996, 2001; Yang and Hatton 2002). However, whether this truly reflects such a scenario is questionable, as dye coupling may be increased by changes in the properties of existing electrical synapses rather than the insertion of new channels. Although an extensive study on the effects of histamine on electrical synapses was not performed in this study, the induction of oscillations by histamine appears to be the result of a network-wide depolarization of already-coupled SPNs, and the associated histamine-induced increase in neuronal input resistance underlies the observed increase in the amplitude of oscillations, rather than histamine having a direct action on electrical synapses themselves. A similar mechanism has been proposed for the feeding peptide orexin in SPNs (van den Top et al. 2003).

CONCLUSIONS

Approximately two thirds of SPNs express histamine H_1 receptor mRNA and are excited by histamine acting through activation of H_1 receptors, leading to the closure of one or more resting leak K^+ conductances. Furthermore, histamine-induced depolarization of electrotonically coupled SPN leads to the induction of membrane potential oscillations, indicative of activation of coupled networks of these neurons. Further studies are required to clarify the functional significance of histamine activation of coupled networks of SPNs and their role in regulating sympathetic drive.

ACKNOWLEDGMENTS

This research was funded by British Heart Foundation (BHF) and the Biotechnology and Biological Sciences Research Council (BBSRC), United Kingdom.

REFERENCES

Agulló L, Picatoste F, and Garcia A. Histamine stimulation of cyclic AMP accumulation in astrocyte-enriched and neuronal primary cultures from rat brain. *J Neurochem* 55: 1592–1598, 1990.

Akins VF and Bealer SL. Hypothalamic histamine release, neuroendocrine and cardiovascular responses during tuberomammillary nucleus stimulation in the conscious rat. *Neuroendocrinology* 57(5): 849–855, 1993.

Brown RE, Stevens DR, and Haas HL. The physiology of brain histamine. *Prog Neurobiol* 63: 637–672, 2001.

Christian EP and Weinreich D. Presynaptic histamine H1 and H3 receptors modulate sympathetic ganglionic synaptic transmission in the guinea-pig. *J Physiol* 457: 407–430, 1992.

Christian EP, Undem BJ, and Weinreich D. Endogenous histamine excites neurones in the guinea-pig superior cervical ganglion *in vitro*. *J Physiol* 409: 297–312, 1989.

Coote JH. The organisation of cardiovascular neurons in the spinal cord. *Rev Physiol Biochem Pharmacol* 110: 147–285, 1988.

Gatti PJ and Gertner SB. The effect of a vasopressin antagonist on the pressor response to histamine administered centrally. *Neuropharmacology* 22(7): 895–902, 1983.

Guo J and Schofield GG. Histamine inhibits KCNQ2/KCNQ3 channel current via recombinant histamine H(1) receptors. *Neurosci Lett* 328(3): 285–288, 2002.

Haas H and Panula P. The role of histamine and the tuberomammillary nucleus in the nervous system, *Nat Rev Neursci* 4: 121–130, 2003.

Hatton GI and Yang QZ. Ionotropic histamine receptors and H_2 receptors modulate supraoptic oxytocin neuronal excitability and dye coupling. *J Neurosci* 21: 2974–2982, 2001.

Hatton GI and Yang QZ. Synaptically released histamine increases dye coupling among vasopressin neurons of the supraoptic nucleus: mediation by H_1 receptors and cyclic nucleotides. *J Neurosci* 16: 123–129, 1996.

Higashi H, Ueda N, Nishi S, Gallagher JP, and Shinnick-Gallagher P. Chemoreceptors for serotonin (5-HT), acetylcholine (ACh), bradykinin (BK), histamine (H) and gamma-aminobutyric acid (GABA) on rabbit visceral afferent neurons. *Brain Res Bull* 8(1): 23–32, 1982.

Hill SJ. Distribution, properties and functional characteristics of three classes of histamine receptor. *Pharmacol Rev* 42: 45–83, 1990.

Hough LB. Cellular localization and possible functions for brain histamine: recent progress. *Prog Neurobiol* 30: 469–505, 1988.

Inagaki N. Characterization of histamine H_1-receptors on astrocytes in primary cultures: [^{3}H] mepyramine binding studies. *Eur J Pharmacol* 173: 43–51, 1989.

Jafri MS, Moore KA, Taylor GE, and Weinreich D. Histamine H1 receptor activation blocks two classes of potassium current, IK(rest) and IAHP, to excite ferret vagal afferents. *J Physiol* 503: 533–546, 1997.

Klein MC and Gertner SB. Studies on the mechanism of the cardiovascular action of central injections of histamine. *Neuropharmacology* 22(9): 1109–1115, 1983.

Klein MC and Gertner SB. Evidence for a role of endogenous histamine in central cardiovascular regulation: inhibition of histamine–N-methyltransferase by SKF 91488. *J Pharmacol Exp Ther* 216(2): 315–320, 1981.

Knigge U, Matzen S, and Warberg J. Histamine as a neuroendocrine regulator of the stress-induced release of peripheral catecholamines. *Endocrinology* 126(3): 1430–1434, 1990.

Leal-Cardoso H, Koschorke GM, Taylor G, and Weinreich D. Electrophysiological properties and chemosensitivity of acutely isolated nodose ganglion neurons of the rabbit. *J Auton Nerv Syst* 45(1): 29–39, 1993.

Leurs R, Traiffort E, Arrang JM, Tardivel-Lacombe J, Ruat M, and Schwartz JC. Guinea pig histamine H_1 receptor. II. Stable expression in Chinese hamster ovary cells reveals the interaction with three major signal transduction pathways. *J Neurochem* 62: 519–527, 1994.

Li Z and Hatton GI. Histamine-induced prolonged depolarization in rat supraoptic neurons: G-protein-mediated, Ca^{2+}-independent suppression of K^+ leakage conductance. *Neuroscience* 70(1): 145–158, 1996.

Liu C, Ma X, Jiang X, Wilson SJ, Hofstra CL, Blevitt J, Pyati J, Li X, Chai W, Carruthers N, and Lovenberg TW. Cloning and pharmacological characterization of a fourth histamine receptor (H(4)) expressed in bone marrow. *Mol Pharmacol* 59: 420–426, 2001.

Logan SD, Pickering AE, Gibson IC, Nolan MF, and Spanswick D. Electrotonic coupling between rat sympathetic preganglionic neurones in vitro. *J Physiol* 495: 491–502, 1996.

Matzen S, Secher H, Knigge U, Bach FW, and Warberg J. Pituitary-adrenal responses to head-up tilt in humans: effect of H_1- and H_2-receptor blockade. *Am J Physiol* 263(1 Pt 2): R156–163, 1992.

McCormick DA and Williamson A. Modulation of neuronal firing mode in cat and guinea pig LGNd by histamine: possible cellular mechanisms of histaminergic control of arousal. *J Neurosci* 11: 3188–3199, 1991.

Mitsuhashi M and Payan DG. Functional diversity of histamine and histamine receptors, *J Invest Dermatol* 98: 8S–11S, 1992.

Munakata M and Akaike N. Regulation of K^+ conductance by histamine H_1 and H_2 receptors in neurons dissociated from rat neostriatum. *J Physiol* 480(2): 233–245, 1994.

Nguyen T, Shapiro DA, George SR, Setola V, Lee DK, Cheng R, Rauser L, Lee SP, Lynch KR, Roth BL, and O'Dowd BF. Discovery of a novel member of the histamine receptor family. *Mol Pharmacol* 59: 427–433, 2001.

Nolan MF, Logan SD, and Spanswick D. Electrophysiological properties of electrical synapses between rat sympathetic preganglionic neurons *in vitro*. *J Physiol* 519(3): 753–764, 1999.

Oda T and Matsumoto S. Identification and characterization of the histamine H_4 receptor, *Nippon Yakurigaku Zasshi* 118(1): 36–42, 2001.

Okuma Y, Yokotani K, Murakami Y, and Osumi Y. Brain histamine mediates the bombesin-induced central activation of sympatho-adrenomedullary outflow. *Life Sci* 61(26): 2521–2528, 1997.

Pickering AE, Spanswick D, and Logan SD. Whole-cell recordings from sympathetic preganglionic neurons in rat spinal cord slices. *Neurosci Lett.* 130: 237–242, 1991.

Reiner PB and Kamondi A. Mechanisms of antihistamine-induced sedation in the human brain: H1 receptor activation reduces a background leakage potassium current. *Neurosci* 59: 579–588, 1994.

Richardson PJ, Dixon AK, Lee K, Bell MI, Cox PJ, Williams R, Pinnock RD, and Freeman TC. Correlating physiology with gene expression in striatal cholinergic neurones. *J Neurochem* 74(2): 839–846, 2000.

Schwartz JC, Arrang JM, Garbag M, Pollard H, and Ruat M. Histaminergic transmission in the mammailian brain. *Physiol Rev* 71: 1–51, 1991.

Shin N, Coates E, Murgolo NJ, Morse KL, Bayne M, Strader CD, and Monsma FJ Jr. Molecular modeling and site-specific mutagenesis of the histamine-binding site of the histamine H_4 receptor. *Mol Pharm* 62: 38–47, 2002.

Singewald N and Philippu A. Involvement of biogenic amines and amino acids in the central regulation of cardiovascular homeostasis. *TIPS* 17(10): 356–363, 1996.

Snow RW and Weinreich D. Presynaptic and postsynaptic effects of histamine and histamine agonists in the superior cervical ganglion of the rat. *Neuropharmacology* 26(7A): 743–752, 1987.

Spanswick D, Renaud LP, and Logan SD. Bilaterally evoked monosynaptic EPSPs, NMDA receptors and potentiation in rat sympathetic preganglionic neurons in vitro. *J Physiol* 509(1): 195–209, 1998.

Starodub AM and Wood JD. Histamine suppresses A-type potassium current in myenteric neurons from guinea pig small intestine. *J Pharmacol Exp Ther* 294(2): 555–561, 2000.

Takada M, Li ZK, and Hattori T. A direct projection from the tuberomamillary projection to the spinal cord in the rat. *Neurosci Lett* 79: 257–262, 1987.

Tangri KK, Gupta GP, and Vrat S. Role of histamine receptor in mesencephalic nucleus dorsalis raphe in cardiovascular regulation. *N S Arch Pharmacol* 339(5): 557–563, 1989.

Telenius H, Carter NP, Bebb CE, Nordenskjold M, Ponder BA, and Tunnacliffe A. Degenerate oligonucleotide-primed PCR: general amplification of target DNA by a single degenerate primer. *Genomics* 13(3): 718–725, 1992.

Undem BJ and Weinreich D. Electrophysiological properties and chemosensitivity of guinea pig nodose ganglion neurons in vitro. *J Auton Nerv Syst* 44(1): 17–33, 1993.

Undem BJ, Hubbard W, and Weinreich D. Immunologically induced neuromodulation of guinea pig nodose ganglion neurons. *J Auton Nerv Syst* 44(1): 35–44, 1993.

Wada H, Inagaki N, Yamatodani A, and Wanatabe T. Is the histaminergic neuron system a regulatory system for whole-brain activity? *Trends Neurosci* 14: 415–418, 1991.

Wahlestedt C, Skagerberg G, Hakanson R, Sundler F, Wada H, and Watanabe T. Spinal projections of hypothalamic histidine decarboxylase-immunoreactive neurons. *Agents Actions* 16: 231–233, 1985.

van den Top M, Nolan MF, Lee K, Richardson PJ, Buijs RM, Davies CH, and Spanswick D. Orexins induce increased excitability and synchronisation of rat sympathetic preganglionic neurons. *J Physiol*. 549: 809–821, 2003.

Yamatodani A, Inagaki N, Panula P, Itowi N, Watanabe T, and Wada H. Structure and functions of the histaminergic neuron system, *Handbook of Experimental Pharmacology* 97: 243–283, 1991.

Yang QZ and Hatton GI. Histamine H_1-receptor modulation of interneuronal coupling among vasopressinergic neurons depends on nitric oxide synthase activation. *Brain Res* 955: 115–122, 2002.

Yasuda T, Masaki T, Sakata T, and Yoshimatsu H. Hypothalamic neuronal histamine regulates sympathetic nerve activity and expression of uncoupling protein 1 mRNA in brown adipose tissue in rats. *Neuroscience* 125(3): 535–540, 2004.